Iranian Society of Acoustics and Vibration
The 12th International Conference on Acoustics and Vibration ISAV2022
14-15 Dec 2022 Tehran - Iran
Amirkabir University of Technology

Conceptual design of dynamic vibration absorber for mitigation of subway tracks vibration

Ali Jafari[a], Aref Afsharfard[b*]

[a] *B.Sc. student, Mechanical engineering department, Ferdowsi University of Mashhad, Vakil-Abaad Blvd, 9177948974, Mashhad, Iran.*

[b] *Associate professor, Mechanical engineering department, Ferdowsi University of Mashhad, Vakil-Abaad Blvd, 9177948974, Mashhad, Iran.*

** Corresponding author e-mail: afsharfard@um.ac.ir*

Abstract

The vibrations and sounds of the train movement that cause damage to buildings close to the train lines are one of the critical challenges for constructing urban rail lines. The system's vibration causes acoustic noise, and it is necessary to use vibration absorbers or viscose dampers to control it. In this study, a dynamic absorber is presented, which absorbs the vibrations without transferring them to the support and depreciation of sound energy. For this purpose, modal analysis of rail track has been done, and vibrational behavior of subway track has been investigated. The vibration model of the rail track has been decoupled into four degrees of freedom system. The similarity of mode shapes obtained from the experimental test and gained from modal analysis indicates the accuracy of the presented vibration model. According to the theories expressed and optimization in MATLAB, the optimal parameters for vibration absorber has been investigated. It is shown that utilizing an absorber can mitigate rail sound and vibration.

Keywords: Modal analysis; Vibration mitigation; Dynamic vibration absorber; subway track.

1. Introduction

One of the essential criteria for the safety and quality of rail transport is the quality of railway lines. Line vibrations are critical in studying the quality factors of railway lines. One of the efficient methods of modeling rails and railway structures is using modal analysis to eliminate or reduce these vibrations of railway lines. Modal testing involves measuring FRFs or structural impact response. FRF measurement can be done by applying a force (measured) at one point in the structure without other excitation forces and measuring the vibration response at one or more points in the system [1, 2, 3]. Vibrational modeling of rails has been done in different ways and has been studied

in many types of research [4, 5]. The vertical dynamic response in a train crossing bridge using modal analysis by combining numerical is investigated [6, 7].

Various methods have been used to improve the performance of structures against dynamic forces. One approach in recent years for reinforcing structures is using energy-absorbing systems, which reduce the displacement of the structure to the desired level. It is used to reduce or eliminate unwanted vibrations.

Tuned mass dampers are a versatile vibration tool in bridge engineering [8]. TMDs in the foundations of a tall building can also reduce wind or earthquake vibrations [9].

Other methods to mitigate vibrations include viscoelastic dampers (VD) and friction pendulum dampers (FPB). The bridge of the railway shows that the TMD attenuator is the best absorber of earthquake vibrations and forced vibration than VD or FPB [10, 11, 12].

This study investigates the vibration model of the subway rail and vibration mitigation of entering the ground. Consequently, using the impact test and modal analysis method, the vibrational behavior of the rail and its mathematical modeling have been investigated. Finally, the conceptual dynamic vibration absorber (DVA) is presented to reduce the buildings' vibrations.

2. Experimental test

In the first step, experimental testing equipment called EMA (Experimental Modal Analysis) was used to perform vibration testing on the part of the subway rail. The following figure shows a schematic view of the test and testbed with shock stimulation.

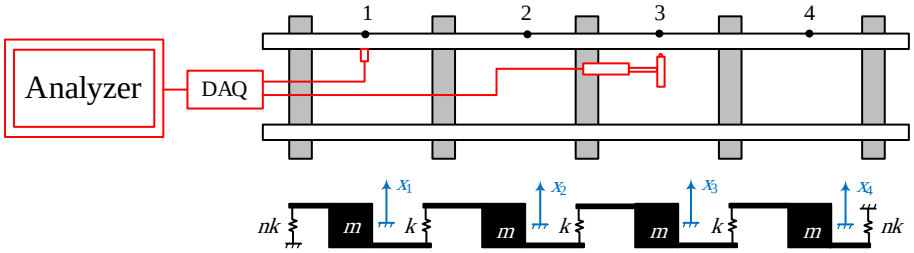

Figure 1: A schematic view of the vibration test and the model equivalent to the mass and spring of the system.

(a) **(b)**

Figure 2: (a) EMA modal testbed on a three-meter rail; (b) Modal test performed by impact shock excitation on rail

The vibration test results in the MeScope software platform can be seen in the figure below. These results include the frequency response of Accelerance and are a combination of point FRF and Transfer FRF, which can be ensured due to the resonance and anti-resonance in the presented figures. The values of the imaginary peaks of the system acceleration response in the first six natural

frequencies of the rail are as described in the table below. It is worth noting that these values can be used to plot the vibration modes of the system.

Table 1: The imaginary term of the peaks of the acceleration curve in the range of the first six natural frequencies

ω (Hz)	438	604	771	980	1210	1456
A_{11}	+0.0398	+0.0489	+0.1150	+0.2520	+0.2740	+0.3090
A_{12}	-0.0148	-0.0476	+0.0143	+0.2450	+0.2390	+0.0990
A_{13}	+0.0368	-0.0370	-0.0753	+0.2330	+0.0284	-0.0829
A_{14}	-0.0385	+0.0606	-0.0787	+0.0656	+0.0880	-0.1060

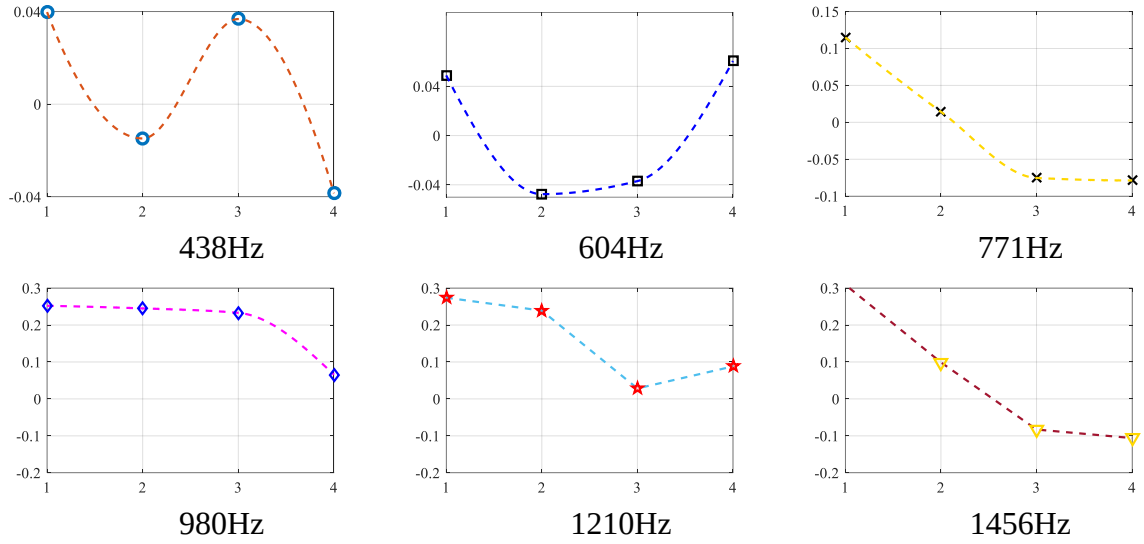

Figure 3: mode shapes of the points shown by the rail in the face of the first six frequencies (experimental)

3. Mathematical modeling

In the above figures, the corresponding modes with lower frequencies lead to the behavior of flexural vibrations in the beam. These types of vibrations are difficult to reduce by rail constraints. However, the modes corresponding to the higher frequencies correlate with the rigid modes. These modes occur due to the lack of rigid connection of the rail to the ground (concreting the foundation). According to the mentioned cases, the first four vibration modes have been used to extract the Lumped model of the continuous vibration system of the rail.

$$\boldsymbol{\Phi} = \begin{bmatrix} +2.52a & +1.15b & +4.89c & +3.98d \\ +2.45a & +0.14b & -4.76c & -1.48d \\ +2.33a & -0.75b & -3.70c & +3.68d \\ +0.66a & -0.79b & +6.06c & -3.85d \end{bmatrix} \quad (1)$$

According to the extracted modal matrix and the principle of orthogonality of vibrating modes, a relation can be constructed as follows. In this regard, it is necessary to zero all non-diagonal arrays. Also, according to the form of considering the points considered for degrees of freedom, all dimensions on the diameter must be equal. Therefore, six equations and three unknowns will be obtained, from which answers will be chosen that bring non-diagonal arrays closer to zero. Finally, the above process can be followed as follows:

$$M = \phi^{-T} I \phi^{-1} \quad (2)$$

$$K = \phi^{-T} \omega^2 \phi^{-1} \quad (3)$$

On the other hand, with the help of natural frequencies and considering the discrete figure shown, the effects of the ***n*** factor on natural frequencies and finally, the frequency ratio error can be extracted as follows:

$$\text{Error} = \sum_{i=1}^{n}\left(\left|\frac{\omega_1}{\omega_i}\right|_{\text{Exp}} - \frac{\omega_1}{\omega_i}\Big|_{\text{Th}}\right) \quad ; \quad n = \text{DOF} \tag{4}$$

Regarding the data presented in this study, the lowest error occurred at n = 2.3. The error changes can be seen in part (b) of the figure below.

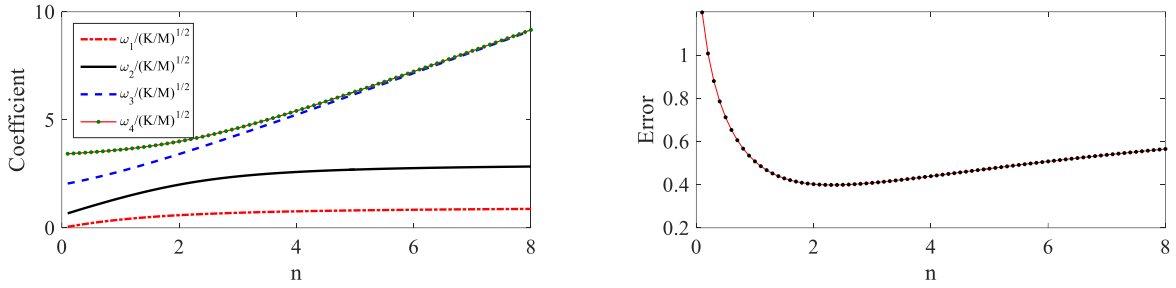

(a) **(b)**

Figure 4: (a) Effects of coefficient ***n*** on natural frequencies; (b) Error of comparing frequencies with coefficient change

According to the display of the system's equivalent mass and spring model, stiffness and mass matrices will be extracted as follows.

$$\mathbf{K} = K\begin{bmatrix} 1+n & -1 & 0 & 0 \\ -1 & 2 & -1 & 0 \\ 0 & -1 & 2 & -1 \\ 0 & 0 & -1 & 1+n \end{bmatrix} \tag{5}$$

$$\mathbf{M} = M\begin{bmatrix} 1 & 0 & 0 & 0 \\ 0 & 1 & 0 & 0 \\ 0 & 0 & 1 & 0 \\ 0 & 0 & 0 & 1 \end{bmatrix} \tag{6}$$

Considering the first four frequencies, the value of $(\frac{\mathbf{K}}{\mathbf{M}})^{1/2}$ on average will equal 2904 radians per second. In this case, the natural frequencies of the system will be as follows:

$$\omega_1 = 2297\frac{\text{rad}}{\text{s}} = 366\text{Hz} \rightarrow \text{Error} = 16\% \qquad \omega_3 = 5567\frac{\text{rad}}{\text{s}} = 886\text{Hz} \rightarrow \text{Error} = 15\%$$

$$\omega_2 = 4246\frac{\text{rad}}{\text{s}} = 676\text{Hz} \rightarrow \text{Error} = 12\% \qquad \omega_4 = 5924\frac{\text{rad}}{\text{s}} = 943\text{Hz} \rightarrow \text{Error} = 4\%$$

The mass of each of the presented rails is equal to 166 kg, and with the object separation technique, M can be considered equal to 41.5 kg with reasonable accuracy. Therefore, according to the results obtained in the previous sections, the value of K will be equal to 349978 $(\frac{KN}{m})$. The mass and stiffness matrices of the system can be displayed as follows:

$$\mathbf{K} = \begin{bmatrix} 1154927 & -349978 & 0 & 0 \\ -349978 & 699956 & -349978 & 0 \\ 0 & -349978 & 699956 & -349978 \\ 0 & 0 & -349978 & 1154927 \end{bmatrix} \times 10^3 \frac{\text{N}}{\text{m}} \tag{7}$$

$$\mathbf{M} = \begin{bmatrix} 41.5 & 0 & 0 & 0 \\ 0 & 41.5 & 0 & 0 \\ 0 & 0 & 41.5 & 0 \\ 0 & 0 & 0 & 41.5 \end{bmatrix} \text{kg} \tag{8}$$

The results are improved in the next step according to the stiffness modification technique.

$$\left([H(\omega^*)][\kappa] + \frac{1}{\gamma_k}[I]\right)[Y] = \{0\} \tag{9}$$

Moreover, the matrix κ is assumed to be as follows:

$$\kappa = \begin{bmatrix} 0 & 0 & 0 & 0 \\ 0 & +1 & -1 & 0 \\ 0 & -1 & +1 & 0 \\ 0 & 0 & 0 & 0 \end{bmatrix} \tag{10}$$

By observing the above assumption and performing operations to correct the second natural frequency, the values of the natural frequencies of the updated system will be as follows:

$$\omega_1 = 1977\frac{\text{rad}}{\text{s}} = 315\text{Hz} \rightarrow \text{Error} = 28\% \qquad \omega_3 = 4843\frac{\text{rad}}{\text{s}} = 771\text{Hz} \rightarrow \text{Error} = 0\%$$

$$\omega_2 = 3737\frac{\text{rad}}{\text{s}} = 594\text{Hz} \rightarrow \text{Error} = 1\% \qquad \omega_4 = 5666\frac{\text{rad}}{\text{s}} = 901\text{Hz} \rightarrow \text{Error} = 8\%$$

In the next step, the results are improved according to the mass modification technique.

$$\left(\omega^{*2}[H(\omega^*)][\varepsilon] - \frac{1}{\zeta_m}[I]\right)[Y] = \{0\} \tag{11}$$

The first step of modifying the mass matrix by considering ε as follows:

$$\varepsilon = \begin{bmatrix} 1 & 0 & 0 & 0 \\ 0 & 0 & 0 & 0 \\ 0 & 0 & 0 & 0 \\ 0 & 0 & 0 & 1 \end{bmatrix} \tag{12}$$

Assuming the above, the result of the mass modification process, taking into account the improvement of the second natural frequency, will result in the values of the natural frequencies as follows:

$$\omega_1 = 2539\frac{\text{rad}}{\text{s}} = 404\text{Hz} \rightarrow \text{Error} = 7.7\% \qquad \omega_3 = 4565\frac{\text{rad}}{\text{s}} = 726\text{Hz} \rightarrow \text{Error} = 5.8\%$$

$$\omega_2 = 4000\frac{\text{rad}}{\text{s}} = 637\text{Hz} \rightarrow \text{Error} = 5.5\% \qquad \omega_4 = 6097\frac{\text{rad}}{\text{s}} = 970\text{Hz} \rightarrow \text{Error} = 1.1\%$$

As seen in the above cases, the maximum error of natural frequencies in all frequencies reached the desired range below 8% of the error. Therefore, the relevant results can be used to continue the calculations. Hence, the development of modifying the stiffness and mass matrices will be as follows*:*

$$\mathbf{K} = \begin{bmatrix} 1154927 & -349978 & 0 & 0 \\ -349978 & 583733 & -23755 & 0 \\ 0 & -23755 & 369372 & -135587 \\ 0 & 0 & -135587 & 940536 \end{bmatrix} \times 10^3 \ \frac{\text{N}}{\text{m}} \tag{13}$$

$$\mathbf{M} = \begin{bmatrix} 54.4 & 0 & 0 & 0 \\ 0 & 22.7 & 0 & 0 \\ 0 & 0 & 22.7 & 0 \\ 0 & 0 & 0 & 54.4 \end{bmatrix} \text{kg} \tag{14}$$

The mode shapes corresponding to the mass and stiffness matrices obtained are as follows. The similarity of this shape of the modes with the items obtained from the experimental test indicates the accuracy of the vibration model presented.

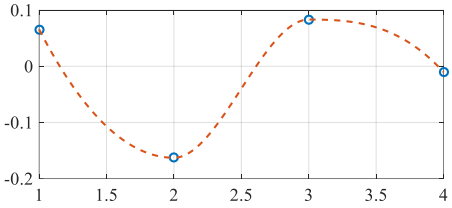

404Hz

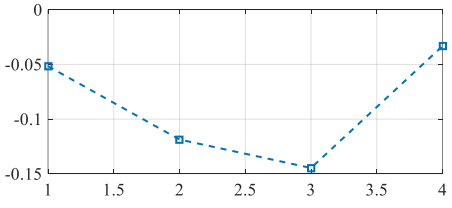

637Hz

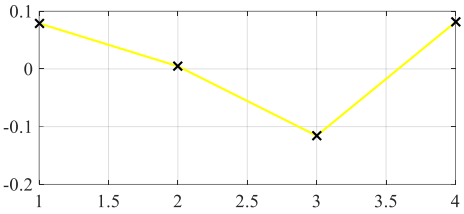

726Hz

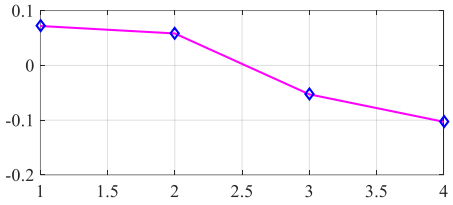

970Hz

Figure 5: mode shapes of the system corresponding to the first four natural frequencies (theory)

Therefore, the modal matrix of the system can be represented as follows:

$$\boldsymbol{\Phi} = \begin{bmatrix} -0.0517 & 0.0720 & -0.0788 & -0.0657 \\ -0.1187 & 0.0584 & -0.0046 & 0.1629 \\ -0.1447 & -0.0528 & 0.1159 & -0.0832 \\ -0.0333 & -0.1030 & -0.0810 & 0.0104 \end{bmatrix} \tag{15}$$

The damping matrix is extracted to ensure the stiffness and mass matrices are acceptable. Therefore, Riley damping is used, and according to this method:

$$\mathbf{C} = a_0\mathbf{M} + a_1\mathbf{K} \tag{16}$$

$$\begin{Bmatrix} a_0 \\ a_1 \end{Bmatrix} = \frac{2\zeta}{\omega_n + \omega_m} \begin{Bmatrix} \omega_n\omega_n \\ 1 \end{Bmatrix} \tag{17}$$

Considering the median of the natural frequencies and the contribution to the attenuation that has been extracted for the vibration test, it is equal to 0.0088 can write*:*

$$\mathbf{C} = 34.4\mathbf{M} + 2.04 \times 10^{-6}\mathbf{K} = \begin{bmatrix} 7207 & -1617 & 0 & 0 \\ -1617 & 3478 & -1080 & 0 \\ 0 & -1080 & 2487 & -626 \\ 0 & 0 & -626 & 6217 \end{bmatrix} \frac{\text{N.s}}{\text{m}} \tag{18}$$

Next, to design a dynamic vibration absorber, it is first necessary to rewrite the system as a separate system. The system's frequency response is the sum of its components. This process will be done using the Decomposition technique as follows*:*

$$H_{ij} = \sum \frac{rA_{jk}}{\omega_r^2 - \omega^2} \tag{19}$$

Therefore, it can be written:

$$H_{11} = \frac{2.673 \times 10^{-3}}{6.446 \times 10^{6} - \omega^2} + \frac{14.089 \times 10^{-3}}{16 \times 10^{6} - \omega^2} + \frac{2.094 \times 10^{-3}}{20.839 \times 10^{6} - \omega^2} + \frac{1.109 \times 10^{-3}}{37.173 \times 10^{6} - \omega^2} \tag{20}$$

In this case, the frequency response can be provided as follows. Then, the equivalent lumped model to each components frequency response can be obtained, which corresponds to one of the natural frequencies of the system:

$$H = -20\log(K) \quad ; \quad \omega \ll \omega_n \tag{21}$$

$$H = -20\log(M) - 40\log(\omega) \quad ; \quad \omega \gg \omega_n \tag{22}$$

Then, using the peak-picking method and considering the fraction of 3 decibels in order to find the side frequencies, with the helping of the following interface, the damping ratio and consequently the damping coefficient can be obtained:

$$\zeta = \frac{\omega_2 - \omega_1}{2\omega_n} \tag{23}$$

Therefore, one-degree of freedom equivalent systems for each degree of freedom can be written as the cases presented in the table below.

Table 2: Specification method of one DOF corresponding to each of the system frequencies

Parameters	Part 1	Part 2	Part 3	Part 4

K (N/m)	851.14×10^6	851.14×10^6	8035.26×10^6	29853.83×10^6
M (kg)	132.34	51.58	385.75	803.36
C (N.s/m)	661.7	309.48	514.3	1606.7

4. Design methodology of DVA

In tuned mass dampers, ample space must be considered for their free displacement due to the relatively large displacement of excess mass in heavy structures attached to these masses. Also, the adsorbent mass in this type of damper is usually less than five percent of the main structure's dynamic mass. In this case, the equations of motion of the system of two degrees of freedom are as follows:

$$M\ddot{x}_1 + Kx_1 + k(x_1 - x_2) = F(t) \quad (24)$$

$$m\ddot{x}_2 + k(x_2 - x_1) = 0 \quad (25)$$

The primary purpose of adding the adsorber is to reduce the range of motion of the structure. The amplitude of the structural vibrations at the resonant frequency will be zero. Therefore, the parameter of the dynamic absorber can be found from the below relations:

$$r_1{}^2, r_2{}^2 = \left(1+\frac{\mu}{2}\right) \mp \sqrt{\left(1+\frac{\mu}{2}\right)^2 - 1} \qquad r_1 = \frac{\Omega_1}{\omega_2} \qquad r_2 = \frac{\Omega_2}{\omega_2} \quad \mu = \frac{m}{M} \quad (26)$$

According to the relationships and theories expressed and simulations performed in MATLAB software, the optimal results in the natural frequency of the third rail for the design of vibration absorbers can be seen in table (3).

Table 3: Specifications of DVA designed using MATLAB software

Ω_1	Ω_2	K	M	μ	r_1	R_2
3910.2 rad/s	4219.9 rad/s	1.04×10^6 N/m	0.3 kg	0.006	0.96	1.04

5. Result and discussion

The vibration absorbers contain a cantilever beam with tip mass at the end of it. Furthermore, a box for holding the beam and installing the DVA on the rail. Experimental testing on the system shows that by using only one unit of DVA on the rail, the frequency response of the rail is as shown in the figure below.

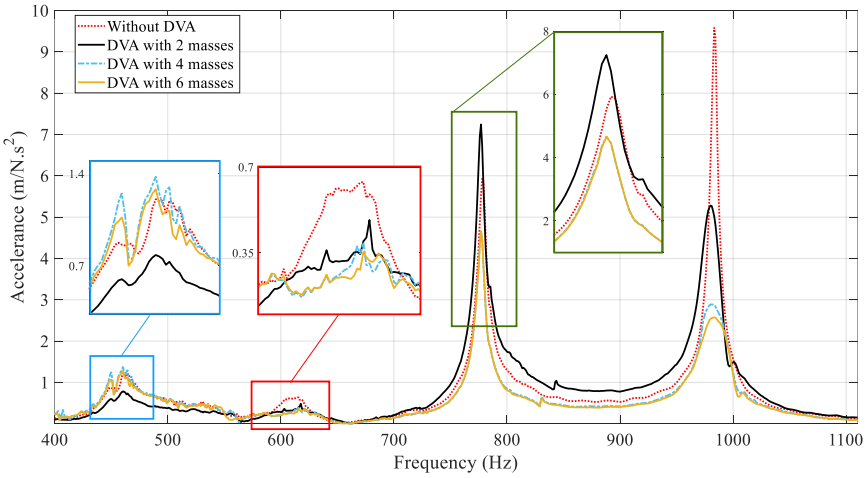

Figure 6: Frequency response of rails by applying DVA and by changing adsorber mass

Adding a DVA with two mass units (meaning the 63 gram) works well at low frequencies but has a reverse performance at the third frequency and increases the amplitude of the vibrations. According to the results and considering the dimensions of the absorber holding box, the number of 6 units of mass, while maintaining all the specifications provided in the construction drawings, will lead to a good performance in reducing the amplitude of vibrations. In the case of a DVA with six additional mass units, except at the first frequency, where the absorber has practically no specific function, In all three other frequencies, we see a reduction in the amount of unwanted vibration of the rail between 22% and 74%.

6. Conclusion

The vibrations and sounds of the train movement that cause damage to buildings close to the train lines are one of the critical challenges for constructing urban rail lines. In this study, a dynamic absorber is presented, which prevents energy transfer to the bed by absorbing the vibrations without transferring it to the support and depreciation of sound energy. It is shown that an absorber can mitigate rail sound and vibration from 22% to 74%. Therefore, installing these absorbers on the rails prevents the vibrations from being transferred to tight urban train lines.

REFERENCES

1. Fu, Zhi-Fang, and Jimin He. *Modal analysis*. Elsevier, 2001.
2. Ewins, David J. *Modal testing: theory, practice and application*, John Wiley & Sons, 2009.
3. Aref Afsharfard, Ali Jafari, Yousef Ayoubi Rad, Haniyeh Tehrani & Kyung Chun Kim, Modifying Vibratory Behavior of the Car Seat to Decrease the Neck Injury, *Journal of Vibration Engineering & Technologies*, 2022.
4. A. Remennikov & S. Kaewunruen, Experimental Investigation on Dynamic Railway Sleeper/Ballast Interaction, *Experimental Mechanics*, 2006.
5. Miguel Aizpun, Asier Alonso & Jordi Vinolas, A new parameter identification methodology for a modal analysis test of a rail vehicle, *Vehicle System Dynamics*, 2014.
6. Ping Lou, Vertical dynamic responses of a simply supported bridge subjected to a moving train with two-wheelset vehicles using modal analysis method, *International Journal for Numerical Methods in Engineering*, 2005.
7. N.F.Nangoloa, J.Soukupa, L.Rychlíkováa & J.Skočilasb, A combined numerical and modal analysis on vertical vibration response of railway vehicle, *Procedia Engineering*, 2014.
8. Zhaowei Chen, Hui Fang, Zhaoling Han & Shizheng Sun, Influence of bridge-based designed TMD on running trains, *Journal of Vibration and Control*, 2019.
9. Takuya Hashimoto, Kohei Fujita, Masaaki Tsuji & Izuru Takewaki, Innovative base-isolated building with large mass-ratio TMD at basement for greater earthquake resilience, *Future Cities & Environment*, 2015.
10. Z. Chen, Zhaoling Han, H. Fang & Kai Wei, Seismic vibration control for bridges with high-piers in Sichuan-Tibet Railway, *Structural Engineering and Mechanics*, 2018.
11. Z. Chen, Zhaoling Han, Wanming Zhai & Jizhong Yang, TMD design for seismic vibration control of high-pier bridges in Sichuan–Tibet Railway and its influence on running trains, *VEHICLE SYSTEM DYNAMICS*, 2018.
12. Jianzhong Li, Mubiao Su & Lichu Fan, Vibration Control of Railway Bridges under High-Speed Trains Using Multiple Tuned Mass Dampers, *JOURNAL OF BRIDGE ENGINEERING*, 2005.